Journal of
Plankton Research

academic.oup.com/plankt

J. Plankton Res. (2019) 41(5): 621–639. First published online October 14, 2019 doi:10.1093/plankt/fbz045

ORIGINAL ARTICLE

Drivers of nano- and microplanktonic community structure in a Patagonian tidal flat ecosystem

JUAN F. SAAD[1,2,3,*], MAITE A. NARVARTE[1,2,3], MARIZA A. ABRAMETO[4] AND VIVIANA A. ALDER[3,5,6]

[1]LABORATORIO DE BIODIVERSIDAD Y SERVICIOS ECOSISTÉMICOS, DEPARTAMENTO DE BIOLOGÍA, ESCUELA SUPERIOR DE CIENCIAS MARINAS, UNIVERSIDAD NACIONAL DEL COMAHUE, SAN MARTIN 247, SAN ANTONIO OESTE 8520, RÍO NEGRO, ARGENTINA. [2]CENTRO DE INVESTIGACIÓN APLICADA Y TRANSFERENCIA TECNOLÓGICA EN RECURSOS MARINOS ALMIRANTE STORNI (CIMAS), GÜEMES 1030, SAN ANTONIO OESTE 8520, RÍO NEGRO ARGENTINA. [3]CONSEJO NACIONAL DE INVESTIGACIONES CIENTÍFICAS Y TÉCNICAS (CONICET), GODOY CRUZ 2290, CIUDAD AUTÓNOMA DE BUENOS AIRES 1425, ARGENTINA. [4]LABORATORIO DE CONTAMINACIÓN AMBIENTAL, UNIVERSIDAD NACIONAL DE RÍO NEGRO, SEDE ATLÁNTICA, DON BOSCO Y LELOIR AV., VIEDMA 8500, RÍO NEGRO, ARGENTINA. [5]LABORATORIO DE ECOLOGÍA MARINA MICROBIANA, DEPARTAMENTO DE ECOLOGÍA, GENÉTICA Y EVOLUCIÓN, FACULTAD DE CIENCIAS EXACTAS Y NATURALES, IEGEBA (UBA-CONICET), UNIVERSIDAD DE BUENOS AIRES, INTENDENTE GÜIRALDES 2160, CIUDAD AUTÓNOMA DE BUENOS AIRES 1428, ARGENTINA. [6]INSTITUTO ANTÁRTICO ARGENTINO, DIRECCIÓN NACIONAL DEL ANTÁRTICO, CERRITO 1248, CIUDAD AUTÓNOMA DE BUENOS AIRES 1010, ARGENTINA.

*CORRESPONDING AUTHOR: jfsaad@gmail.com

Received December 28, 2018; editorial decision July 9, 2019; accepted July 9, 2019

Corresponding editor: John Dolan

Tidal flats are exceptionally dynamic coastal ecosystems. Tides are their main source of energy, whose influence decreases landwards (as land elevation increases), thus shaping physical, chemical and biological gradients. In this study, we assess whether the structure of nano- and microplankton varies along a spatial gradient in San Antonio Bay (SAB, SW Atlantic), a semi-desert coastal ecosystem with a wide tidal flat and a macrotidal regime. We hypothesize that the tidal effect shapes SAB's both taxonomical groups and size spectrum. The seasonal sampling of 9 sites revealed that diatoms and small flagellates were the most abundant groups, together accounting for over 75% of total density in practically all sites and seasons. High densities of meroplanktonic stages of *Ulva lactuca* were recorded in spring at the innermost sites, accounting for over 95% of all planktonic cells. Slopes of the size spectrum analysis were in line with highly productive inshore waters (mean, −0.64) and showed that larger phytoplankton was the main contributor to total biomass, despite its decreasing importance toward inner sites. The spatial and seasonal variations found for lower trophic web compartments provide evidence of the importance of tidal transport in ruling phytoplankton structure in tidal flats under strong macrotidal regimes.

KEYWORDS: Patagonian tidal flat; marine ecosystem; unicellular eukaryotic plankton; size-abundance spectra; species assemblages

available online at academic.oup.com/plankt

INTRODUCTION

Tidal flats are globally widespread and exceptionally dynamic coastal ecosystems considered as crucial for the subsistence of human population all around the world (Murray *et al.*, 2019). However, the status and some distinctive ecological processes and their fluctuations in the spatial and temporal scales are still poorly known for some tidal flats of the world.

Tides and waves are the main source of energy in coastal environments, and their influence typically decreases and increases, respectively, landwards (Friedrichs, 2011). Particularly in coastal tidal flats, the tidal range thrives over the typical wave height (Hayes, 1979). Tidal fluctuations produce the daily movement of a huge amount of water mass that covers and uncovers the intertidal surface of tidal flats and results in environmental gradients whose characteristics depend on ground elevation (Hinde, 1954; Traut, 2005), hydrology (Sanderson *et al.*, 2000; Zedler *et al.*, 1999) and the degree of convexity or concavity of the cross-shore profile (Bearman *et al.*, 2010), among other factors.

The high intertidal zone is rich in organic matter (Tzortziou *et al.*, 2008) and halophytic vegetation associated with marshes. During the flooding process, tides remove nutrients, organic matter and part of the benthic microbial community (Negrin *et al.*, 2011), thus increasing the level of dissolved and particulate matter in the water column. These processes respond to Odum's (1980) outwelling hypothesis, which postulates that coastal environments are net exporters of matter to surrounding maritime areas, thus enhancing its secondary production. Their relevance depends on several interlinked factors like the land's slope (Taylor and Allanson, 1995), geomorphology (Cicchetti and Diaz, 2002), the presence of dams and/or breakwaters (Koch and Gobler, 2009), the tidal regime and amplitude (Kwak and Zedler, 1997; Ibañez *et al.*, 2000) and sporadic events of torrential rains (Odum, 2002) and intense winds (McManus and Woodson, 2012), among others.

In low wave systems, suspended particles are transported by tides from higher to lower energy areas, namely from offshore toward the coast. In this sense, a decrease in the abundance of suspended particle concentrations (and in the magnitude of tidal stress) is expected over the seabed (Friedrichs, 2011). A shift in the size spectrum of suspended particles is also expected landwards, with a progressive impoverishment of larger particles and species as tide energy decreases. In fact, Shimeta and Sisson (1999) verified that the degree of turbulence associated with the flow and reflux phases of tidal currents generates a differential effect on the size, shape, degree of aggregation/disaggregation and vertical migration of plankton. However, it has also been reported that some phytoplanktonic groups with intrinsic capacity to form cell and chain aggregates do not show substantial variation along the tidal cycle (Guinder *et al.*, 2009).

The relative abundance of small and large cells of phytoplankton is a helpful tool to describe the community structure and to draw links between some processes where organisms are involved (e.g. nutrient cycling, light acquisition and sinking) and some ecosystem features (e.g. grazing, biogeochemical cycles and primary productivity) (Acevedo-Trejos *et al.*, 2013 and references therein). Phytoplankton size structure often varies with resource availability and hydrographic conditions; for example, in environments with enriched waters with high flow and low sedimentation rates, larger cells typically account for the bulk of the phytoplankton biomass (Huete-Ortega *et al.*, 2010). Applying size spectrum analysis to planktonic communities along coastal environments with strong fluctuations in their physical and chemical variables often proves to be helpful to disentangle spatial and temporal processes occurring therein (e.g. Quintana *et al.*, 2002; Reul *et al.*, 2005, 2008).

The San Antonio Bay (SAB; 40° 46 S, 64° 54′ W) is a wide tidal flat located within a Patagonian semi-desert coastal ecosystem. The area is characterized by a semidiurnal tidal regime (varying between 6 and 9 m) and the exchange of enormous amounts of water with the San Matías Gulf (SMG) through a relatively small mouth. The semicircular shape of the bay serves as protection against the strong energy of SMG waters and enables the formation of extended tidal flat areas, two main spits and marshes (Carbone *et al.*, 2007). After circulating through the bay during each tidal cycle, the incoming water increases its salinity and its content of nutrients and phytoplankton (Esteves *et al.*, 1996). On the other hand, SAB is subject to anthropogenic disturbances associated with land water discharges and *maritime-related activities* at harbors (Carbone *et al.*, 2007); therefore, it was speculated that the joint effect of tidal flushing and benthic community and recycling of organic matter would be softening the impact on water quality (Martinetto *et al.*, 2010). The study of phytoplankton as bioindicators of pollution together with physical/chemical properties is paramount to track water quality in the area. The few articles available on the SAB plankton deal either with diatom diversity (Sar, 1996a, b) or the impact of urban pollution on the abundance of some phytoplanktonic species (Esteves *et al.*, 1996; Martinetto *et al.*, 2010), and thus the spatial and temporal dynamics of planktonic communities in the area are practically unknown. Such knowledge is essential for understanding the spatial

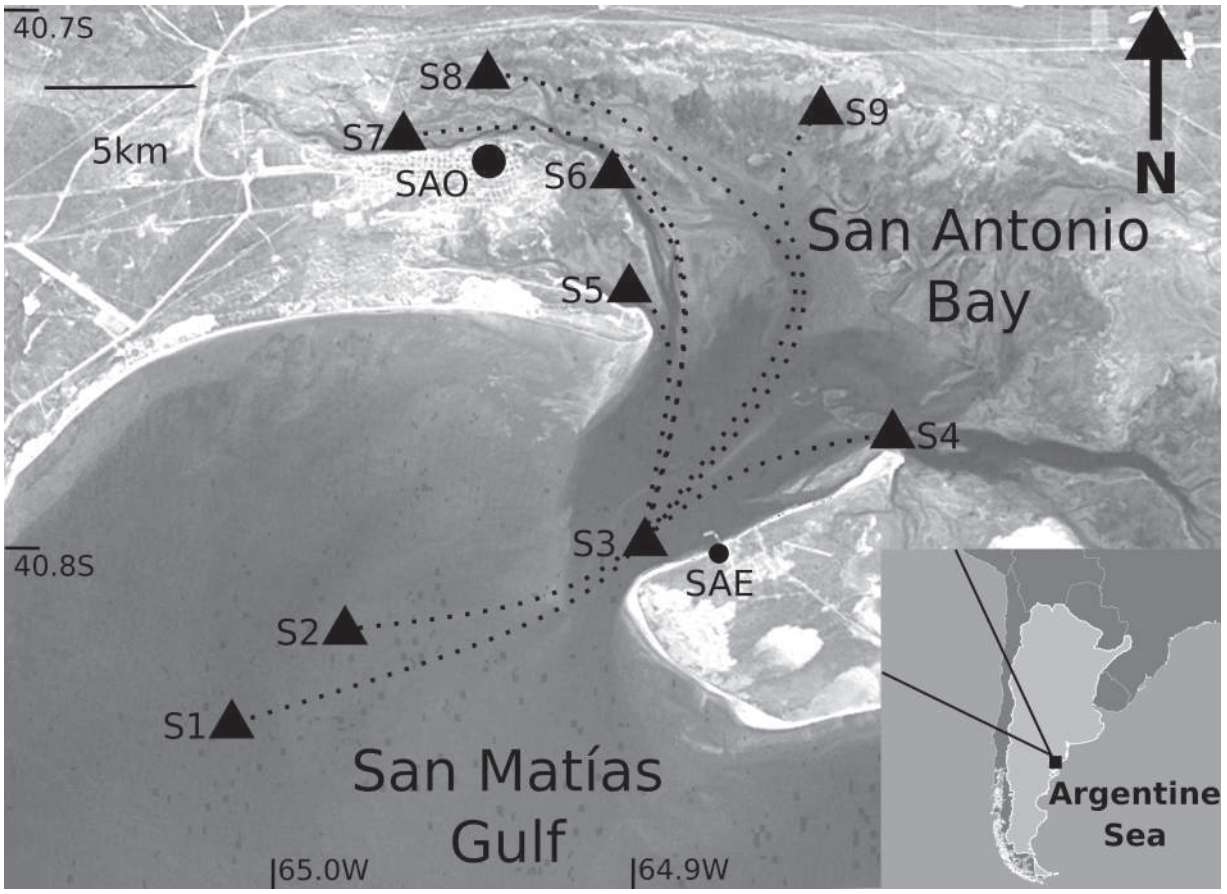

Fig. 1. Location of the studied sites in Bahía San Antonio (North Patagonian waters, Argentina) in 2016 and 2017. SAO, San Antonio Oeste city. SAE, San Antonio Este city. Dotted lines represent distance measurements starting from the mouth of the bay (S3) following the path of water circulation during tidal rising.

patterns of the lower trophic levels, their variations in structure and size with time, the relationships with the dynamics of the SAB tidal flat and, in fine, their ecologic role in the area.

The overall objective of our study is to assess whether there is a variation in nano- and microplankton in terms of taxonomic composition and size structure along the spatial gradient extending from outer SMG waters to the innermost sectors of SAB and whether the trends remain throughout the year. The analysis includes both the environmental setting and the ecological features of various taxa at different distances from the coast.

We hypothesize that (i) the community structure of nano- and microplanktonic organisms is the result of SAB's strong macrotidal regime and that (ii) as the tidal stress decreases from outer gulf waters to the inner parts of the bay, the planktonic community structure becomes less represented by the larger size fractions.

METHOD

Study site and sampling procedure

With an area of 80 km^2, SAB includes tidal flats and channels, spits, beaches and sandbanks. It is dominated by a main channel with a maximum depth of 37 m, toward which a number of secondary tidal channels converge. Spring tides in SAB, with amplitudes of up to 9 m, can generate currents of >2 m seg^{-1}.

To properly describe the land elevation gradient from SMG (outer SAB) across the main channel up to the inner channels of the bay and assess the existence of a coupled environmental and biological gradient, nine different sampling sites were selected (S1–S9) (Fig. 1). A distance value starting from the mouth of the bay (S3) was assigned to each site using the QGIS software (www.qgis.org), following the path of water circulation into the bay during tidal rising. Additionally, ground elevation at each site was measured with GPS. Each site was sampled in

winter (August 2016), summer (February 2017), autumn (May 2017) and spring (October 2017), always at low tide (data from WTides software, www.wtides.com). In autumn, sites S1 and S2 could not be sampled due to logistic issues.

Samples for the analysis of nutrients, chlorophyll *a* (Chl-*a*), colored dissolved organic matter (CDOM), phytoplankton and protozoans (both quantitative and qualitative) were collected from subsurface waters. In the shallowest sites (bottom depth, <1 m; sites S4, S5, S6, S7, S8 and S9; Fig. 1), samples were collected from a 0.5 m depth; in the remaining sites (S1, S2 and S3), the upper 10 m of the water column were sampled by means of a hosepipe sampler with a diameter of 3/4″ (Boltovskoy, 1981; Zohary and Ashton, 1985). *In situ* measurements of temperature and salinity were taken at each site using a multi-parameter probe (YSI 6600-S).

Analysis of water quality variables

The seawater collected at each site was kept cooled until filtration through GF/F filters at the laboratory. Chl-*a* concentration was estimated by first filtering 1.5 L of water and then extracting with acetone for 12 h (Lorenzen, 1967). Measurements were taken with a UV-Vis spectrophotometer (PG Instruments T60), while concentrations were calculated by using Marker's equations (Marker *et al.*, 1980). For the assessment of nutrient concentration, subsamples of filtered water were kept frozen at −20°C. Nitrate and soluble reactive phosphorus (SRP) were estimated by the Nitrate Electrode Method (4500-NO3—D) and the Vanadomolybdophosphoric Acid Colorimetric Method (4500-P—C), respectively (APHA, 2012). Samples for determination of CDOM spectral absorption coefficients were filtered through GF/F filters, and absorption spectra from 200 nm to 800 nm (1 nm data interval) were determined with 1 cm quartz cuvettes and Milli-Q water as the blank, using a double-beam Persee T7S UV-Visible spectrophotometer (Helms *et al.*, 2008). CDOM characterization was obtained through the spectral slope ratio (Sr), a variable inversely correlated to CDOM that is calculated as the spectral slope at 275–295 nm ($S_{275–295}$) divided by the spectral slope at 350–400 nm ($S_{350–400}$), following Hansen *et al.* (2016).

Microscopic analysis

Qualitative samples for the taxonomic identification of nano- and microplankton species were collected by dragging a 15 μm mesh net, fixed with 2–3% formaldehyde and analyzed with an upright microscope at 1000×. Diatoms and dinoflagellates were identified on samples previously cleared with sodium hypochlorite and mounted with Stirax. A total of two slides were observed per sample. Identifications at the species level (whenever possible) were based on descriptions by Balech (1988; dinoflagellates), Sar (1996a, b, diatoms) and Tomas (1997; diatoms and flagellates).

Samples for the quantitative analysis of nano- and microplankton were fixed with 0.4% formaldehyde. The picoplankton was not included in this study. Cell counts were performed under inverted microscope following Utermöhl's (1958) technique, by settling three 10–33 mL aliquots per sample in chambers for >12 hs. The volume of the aliquots was decided as a trade-off between a statistically suitable number of counted individuals and a correct visualization of the samples due to precipitation of inorganic particles masking the cells, an issue that was evident mainly in samples from the inner waters of the bay. Counting errors were estimated according to Venrick (1978), accepting a maximum error of 20% for the most frequent taxa. For nano- and microplankton usually more than 300 and 200 individuals were counted per sample, respectively. Abundance and biovolume estimations were addressed only on individual cells, regardless of whether these were solitary or forming part of a colony or filament (Alder and Morales, 2009).

Taxa were merged into 5 main groups: diatoms, flagellates < 20 μm ("small flagellates"), flagellates > 20 μm (cryptophytes, euglenophytes, silicoflagellates and coccolithophorids), ciliates (loricate and naked) and dinoflagellates. Zoospores of macroalgae were also identified and counted. Total density (ind. mL^{-1}) for each site and season was estimated by adding the individual density of each group.

Cell volume (μm^3) for each group was obtained by first estimating its average dimensions based on the measurement of 20–30 individuals with the aid of ImageJ software and then applying the geometric formula with the best fitting to its cell morphology (Hillebrand *et al.*, 1999; Sun and Liu, 2003). The biovolume per milliliter ($\mu m^3\ mL^{-1}$) for each group was calculated by multiplying each density by its corresponding cell volume. Total biovolume per milliliter ($\mu m^3\ mL^{-1}$) of each sample was calculated by simply adding the biovolumes of all groups present. For better comparison of anisodiametric cell shapes, from cell volume of each taxa, the equivalent spherical diameter (ESD) was calculated as the diameter of a sphere with equivalent volume, according to Taniguchi *et al.* (2014).

Data analysis

Statistical differences of environmental variables between seasons were analyzed using Analysis of Variance

Table I: Spatial and temporal trends of environmental variables from outer waters of SMG to SAB

		Spatial scale			Temporal scale				Mean
		Outer	Intermediate	Inner	Seasons				
Sites/seasons		S1–S3	S4–S6	S7–S9	A	W	S	Su	
Elevation (m)	X	3.0	9.3	11.5					8.2
	±SD	2.6	0.61	0.8					3.8
Distance (m)	X	7.3	18.3	23.4					16.8
	±SD	5.3	1.2	1.4					7.3
Temperature (°C)	X	13.6	14.5	17.1	11.3	12.3	15.8	20.3	15.1
	±SD	3.3	5.3	4.8	1.2	3.2	2.8	4.3	4.7
Salinity	X	33.7	33.7	44.7	37.8	37.3	37.2	38.1	37.6
	±SD	0.7	0.8	11.2	8.9	8.7	8.9	8.6	8.4
SRP (μM)	X	7.6	8.5	42.7	19.6	9.1	30.1	22.3	20.3
	±SD	9.4	6.3	23.6	14.1	16.5	31.4	20.5	22.5
NO_3 (mM)	X	0.9	1.0	1.3	1.0	1.1	1.2	1.0	1.1
	±SD	0.2	0.2	0.3	0.3	0.3	0.3	0.3	0.3
Chl-*a* (ugL^{-1})	X	1.4	1.2	3.5	0.9	0.9	4.4	1.8	2.0
	±SD	1.2	0.5	3.8	0.5	0.4	4.0	1.2	2.6
Sr	X	1.2	1.0	0.9	0.9	1.2	1.0	1.1	1.0
	±SD	0.2	0.2	0.3	0.2	0.1	0.4	0.1	0.3

Sites were grouped in S1–S3 for outer sites, S4–S6 for intermediate sites and S7–S9 for inner sites. SRP, soluble reactive phosphorus; NO_3, dissolved nitrates; Chl-*a*, Chlorophyll a. A, autumn; W, winter; S, spring; Su, summer.

(ANOVA) and *post hoc* Tukey's tests, after verifying assumptions of normality and homoscedasticity with the Shapiro–Wilk and Levene tests, respectively. Ordination of sampling sites according to Chl-*a* concentration, conductivity, temperature and spectral slope ratio (Sr) was achieved by principal component analysis (PCA). Scores for each site on PCA1 axis were used as a synthetic variable to be evaluated together with the spatial variables (distance and elevation) by means of Spearman correlation analysis. Additionally, PCA analyses were conducted with both nano- and microplankton species abundances and biovolumes in order to identify possible differences in species assemblages among sites.

Spearman correlation analyses were also conducted to address correspondence of total density and biovolume with distance, elevation and PCA1. Additionally, log–log analyses by means of simple linear regressions based on both ordinary least square method (OLS) and reduced major axis (RMA) method were performed between log_2-transformed values of each planktonic group's mean size and relative density. Slopes for each site were evaluated together with distance, elevation and PCA1 by means of Spearman correlation analysis. For ease of visualization of the changes in the size spectrum of unicellular plankton across sites, total density and total biovolume were plotted against cell size by considering 6 ESD classes (2–5, 5–10, 10–20, 20–40, 40–80 and <80 μm) (adapted from Marañón, 2014). Statistical tests were performed using IBM SPSS and R software (R Core Team, 2016).

RESULTS

Spatial and environmental trends

Higher values of distance and elevation corresponded to the innermost sites of SAB (S7: 21.7 km, 12.58 m; S8: 23.6 km, 11.1 m; and S9: 24.9 km, 10.88 m, distance and elevation, respectively). Distances of sampling sites were positively correlated to elevation ($R^2 = 0.90$, $P < 0.0001$).

Mean temperatures were found to decrease ~1°C from autumn to winter and to increase ~5°C from spring to summer (Table I). Regardless of the season, water temperature in the inner channels was strongly linked to air temperature due to their shallowness and the extended periods during which these environments remain unaffected by tides. The highest water temperatures were measured at the inner sites (Table I), reaching a maximum of 26.8°C at S7 in summer. Salinity increased landwards, with no statistically significant variation through seasons. Nevertheless, site 9 stood out among the other sites by its extremely high and sustained salinity values (from 57.59 to 60.55) during all seasons.

The nutrient concentrations displayed a rising trend landwards across the flat. Despite the seasonal variations, higher values of nitrates and SRP were always measured at the inner sites (S7–S9; Table I).

Higher Chl-*a* values were registered in the inner sites of the bay (Table I). Differences between seasons were statistically significant (ANOVA, $F_{3;30} = 5.03$, $P = 0.006$), with lower, similar concentrations in winter and autumn (<1 μgL^{-1}), and higher concentrations in summer

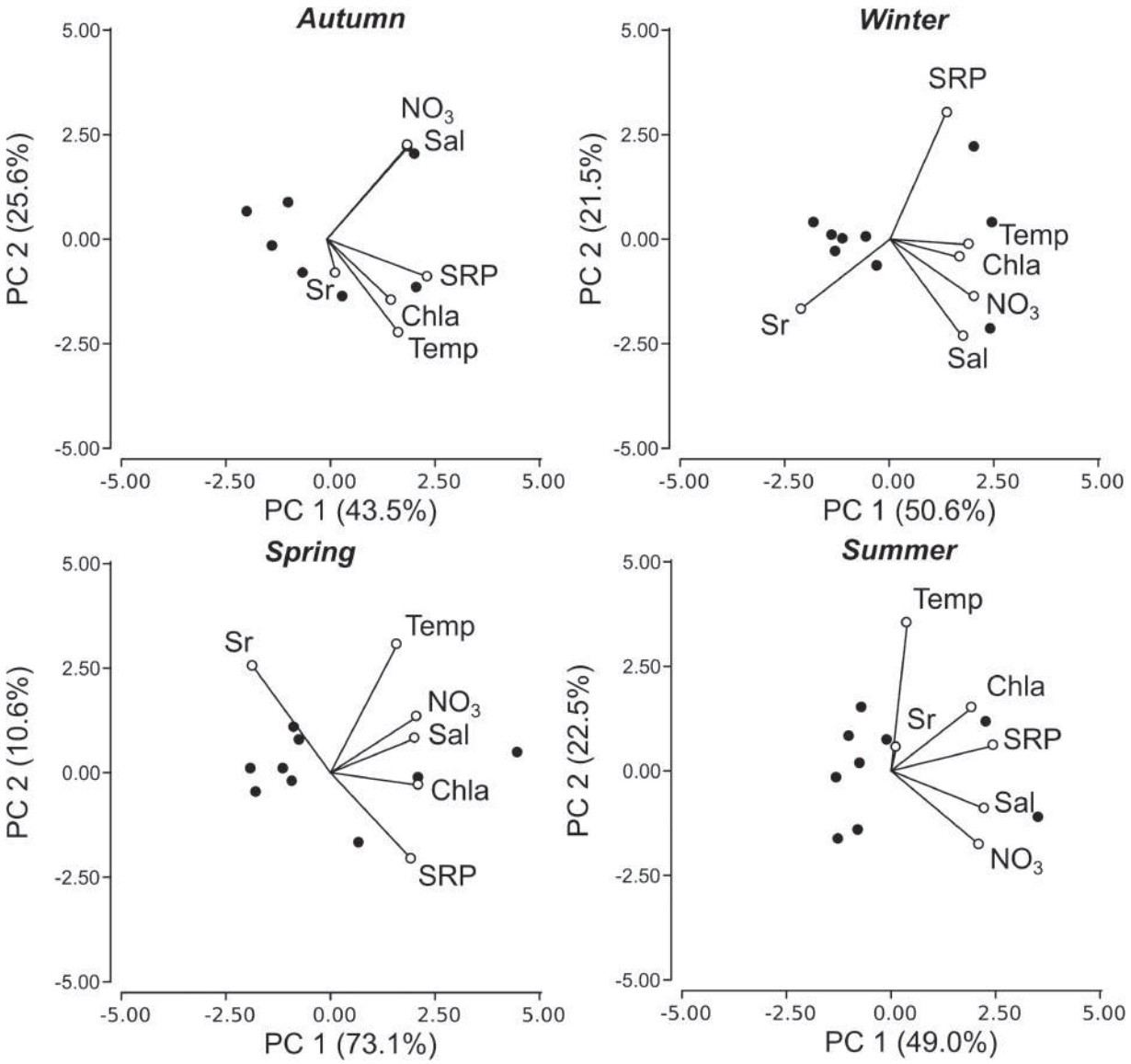

Fig. 2. Ordination plot obtained by a PCA based on the environmental variables measured at San Antonio Bay: SRP, soluble reactive phosphorus; Chla, Chlorophyll *a*; Temp, temperature; Sal, salinity; NO_3, dissolved nitrates; Sr, spectral slope ratio (CDOM). Arrows indicate the loading of each variable on the first two axes. Percentages on each axis indicate the amount of variance explained.

and spring. CDOM concentrations also increased landwards, as evidenced by the lower Sr values in inner channels and the higher ones in outer waters. The lowest Sr values (<0.6) were measured at the inner sites in spring.

Considering the environmental variables per season, axis 1 of the PCA analyses was found to explain a large percentage of the variance (Fig. 2). Chl-*a*, temperature, salinity and nutrients showed a strong positive correlation with PCA1. The spectral slope ratio (Sr) had a low weight in the ordination for autumn and summer and showed a negative correlation with PCA1 for winter and spring. With the exception of autumn, correlations of PCA1 vs. elevation and distance were also highly significant through seasons (Fig 3).

Temporal and spatial trends of nano- and microplankton

The total planktonic density increased in one order of magnitude from the outer SMG waters/mouth of SAB to the inner waters of the bay (Table II), with the highest densities being recorded at sites 7–9. In the temporal scale, total densities differed significantly between seasons

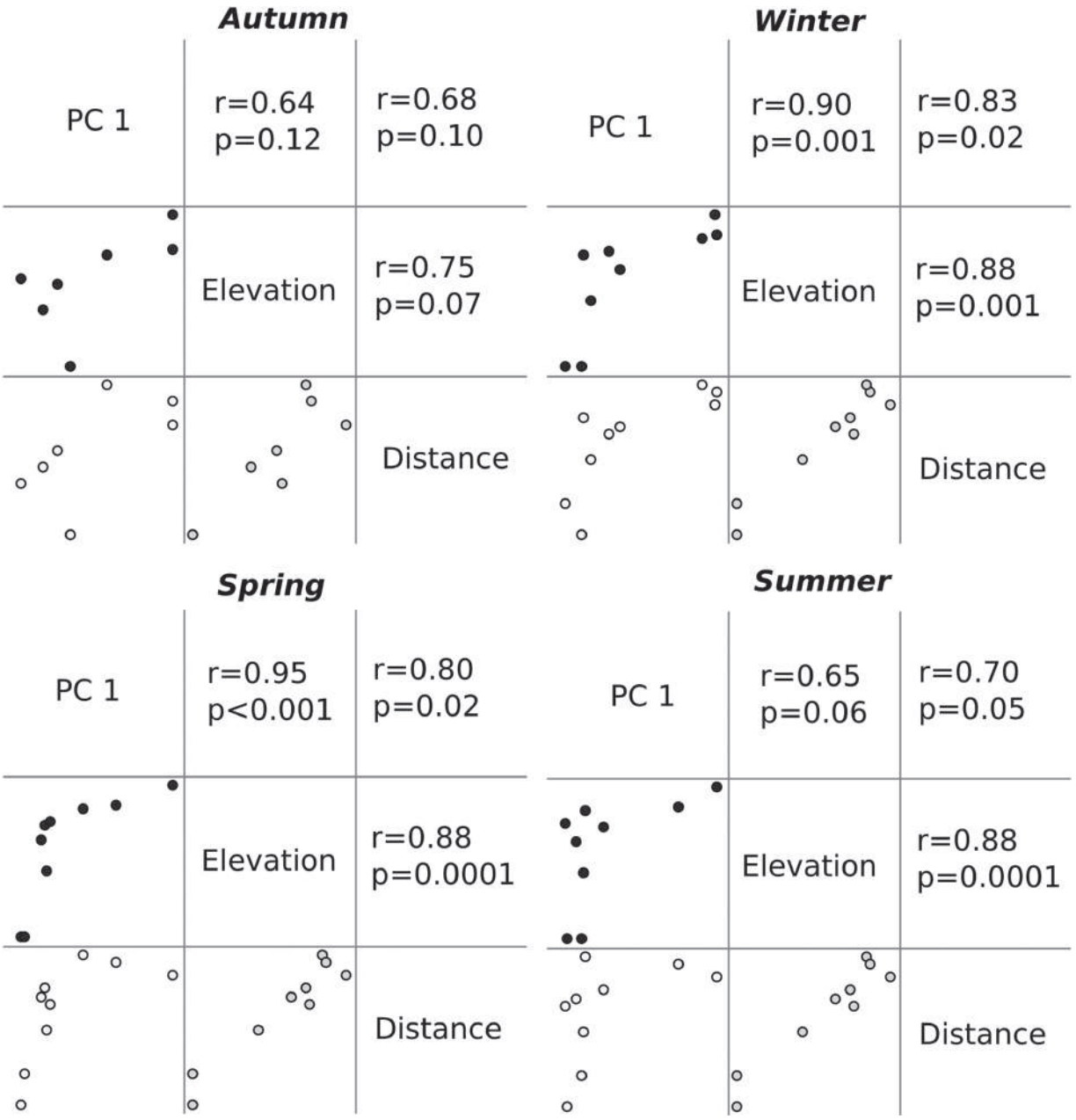

Fig. 3. Correlation of axis 1 scores from PCA (PC 1, Fig. 2) vs. distance and ground elevation of sampling sites in SAB. *r*, Spearman correlation coefficient; *P*, *P*-value for each correlation considering critical value 0.05.

(ANOVA, $F_{3,30} = 4.01$, $P = 0.016$), with the minimum in winter (mean, 7.14×10^2 ind.mL^{-1}), 2 orders of magnitude lower than the maximum of spring (2.0×10^4 ind.mL^{-1}). Summer and autumn reached intermediate mean densities.

The total biovolume was found to significantly increase landwards during spring and summer and decrease significantly in winter. A nonsignificant, although apparent decreasing trend landwards was detected also for autumn. A comparison of total biovolumes between seasons did not yield significant differences (mean, $1.1 \times 10^7 \pm 3.3 \times 10^7$ μm^3 mL^{-1}; ANOVA, $F_{3,30} = 0.75$, $P = 0.53$).

Within each season, both total density and total biovolume (Table III) correlated significantly to at least one of the spatial/environmental variables (distance, elevation and/or PCA1). In particular, total density was positively correlated to PCA1 for all seasons, while both total density

Table II: Spatial and temporal trends of total density (cell mL^{-1}) and total biovolume (μm^3 mL^{-1}), and mean values of the EDS (μm), density (D, cell mL^{-1}) and biovolume (B, μm^3 mL^{-1}) of each planktonic group from outer to inner waters of SAB

		Spatial scale			Temporal scale			
		Outer	Intermediate	Inner	Seasons			
Sites/seasons		S1–S3	S4–S6	S7–S9	A	W	S	Su
Total density		$1.1 \times 10^3 \pm 1.5 \times 10^3$	$1.2 \times 10^3 \pm 1.0 \times 10^3$	$2.0 \times 10^4 \pm 3.6 \times 10^4$	$3.2 \times 10^3 \pm 2.2 \times 10^3$	$7 \times 10^2 \pm 9.1 \times 10^2$	$2.1 \times 10^4 \pm 4.2 \times 10^4$	$6.2 \times 10^3 \pm 8.5 \times 10^3$
Total biovolume		$6.5 \times 10^6 \pm 8.5 \times 10^6$	$2.1 \times 10^6 \pm 8.3 \times 10^5$	$2.4 \times 10^7 \pm 5.4 \times 10^7$	$5.0 \times 10^6 \pm 7.9 \times 10^6$	$5.5 \times 10^6 \pm 6.4 \times 10^6$	$2.9 \times 10^7 \pm 6.2 \times 10^7$	$2.2 \times 10^6 \pm 2.1 \times 10^6$
Diatoms	ESD	29.8 ± 31.7	21.4 ± 12.7	20.8 ± 13.9	22.4 ± 17.06	29.1 ± 29.39	20.7 ± 13.00	20.6 ± 14.37
	D	$1.5 \times 10^3 \pm 1.6 \times 10^3$	$1.2 \times 10^3 \pm 1.0 \times 10^3$	$2.0 \times 10^4 \pm 3.6 \times 10^4$	$3.2 \times 10^3 \pm 2.2 \times 10^3$	$7.1 \times 10^2 \pm 9.1 \times 10^2$	$2.1 \times 10^4 \pm 4.3 \times 10^4$	$6.2 \times 10^3 \pm 8.5 \times 10^3$
	B	$6.0 \times 10^6 \pm 7.2 \times 10^6$	$8.0 \times 10^5 \pm 7.1 \times 10^5$	$1.5 \times 10^6 \pm 1.6 \times 10^6$	$3.0 \times 10^6 \pm 6.2 \times 10^6$	$4.1 \times 10^6 \pm 5.8 \times 10^6$	$1.4 \times 10^6 \pm 1.8 \times 10^6$	$6.8 \times 10^5 \pm 7.0 \times 10^5$
Ciliates	ESD	47.8 ± 2.0	48.5 ± 1.9	48.34 ± 2.0	48.24 ± 2.0	48.06 ± 2.0	48.06 ± 2.1	48.58 ± 2.0
	D	17.5 ± 11.5	7.7 ± 6.7	5.4 ± 4.9	11.8 ± 15	10.8 ± 7.1	6.9 ± 6.7	7.2 ± 4.6
	B	$1.1 \times 10^6 \pm 7.5 \times 10^5$	$4.7 \times 10^5 \pm 4.0 \times 10^5$	$3.2 \times 10^5 \pm 3.0 \times 10^5$	$7.3 \times 10^5 \pm 9.7 \times 10^5$	$6.5 \times 10^5 \pm 4.4 \times 10^5$	$3.9 \times 10^5 \pm 3.8 \times 10^5$	$4.4 \times 10^5 \pm 2.9 \times 10^5$
Dinoflagellates	ESD	51.9 ± 8.1	47.3 ± 9.5	46.2 ± 9.8	53.145 ± 0.02	46.16 ± 9.0	43.38 ± 9.7	54.005 ± 8.6
	D	3.8±4.9	1.5±1.7	4.0±4.3	1.7±1.7	4.4±5.6	3.0±4.1	3.3±3.0
	B	$2.8 \times 10^5 \pm 3.5 \times 10^5$	$9.2 \times 10^4 \pm 1.2 \times 10^5$	$1.9 \times 10^5 \pm 2.2 \times 10^5$	$1.3 \times 10^5 \pm 1.3 \times 10^5$	$2.5 \times 10^5 \pm 3.9 \times 10^5$	$1.0 \times 10^5 \pm 1.0 \times 10^5$	$2.6 \times 10^5 \pm 2.4 \times 10^5$
Flagellates > 20	ESD	23.0 ± 14.5	32.6 ± 26.1	$26.3 \pm$	26.4 ± 19.1	35.2 ± 27.9	25.5 ± 19.3	25.1 ± 17.2
	D	$1.5 \times 10^2 \pm 2.2 \times 10^2$	38.1 ± 51.8	39.7 ± 45.5	$1.5x10^2 \pm 2.5 \times 10^2$	17.4 ± 17.6	2.9 ± 2.9	70.4 ± 41.7
	B	$6.7 \times 10^5 \pm 9.2 \times 10^5$	$3.9 \times 10^5 \pm 5.0 \times 10^5$	$3.1 \times 10^5 \pm 3.3 \times 10^5$	$9.9 \times 10^5 \pm 9.6 \times 10^5$	$1.2 \times 10^5 \pm 1.1 \times 10^5$	$2.8 \times 10^4 \pm 3.7 \times 10^4$	$5.0 \times 10^5 \pm 4.6 \times 10^5$
Flagellates <20um	ESD	2.7 ± 6.2	2.7 ± 6.2	2.7 ± 6.2	2.7 ± 6.2	2.7 ± 6.2	2.7 ± 6.2	2.7 ± 6.2
	D	$9.4 \times 10^2 \pm 8.9 \times 10^2$	$9.7 \times 10^2 \pm 9.7 \times 10^2$	$4.2 \times 10^3 \pm 7.0 \times 10^3$	$1.6 \times 10^3 \pm 9.8 \times 10^2$	$5.0 \times 10^2 \pm 8.0 \times 10^2$	$6.6 \times 10^2 \pm 5.9 \times 10^2$	$5.2 \times 10^3 \pm 7.8 \times 10^3$
	B	$9.4 \times 10^3 \pm 8.9 \times 10^3$	$9.7 \times 10^3 \pm 9.7 \times 10^3$	$4.2 \times 10^4 \pm 7.0 \times 10^4$	$1.6 \times 10^4 \pm 9.8 \times 10^3$	$5.0 \times 10^3 \pm 8.0 \times 10^3$	$6.6 \times 10^3 \pm 5.9 \times 10^3$	$5.2 \times 10^4 \pm 7.8 \times 10^4$
Ulva zoospores	ESD	0	0	14.0 ± 11.3	0	0	14.0 ± 11.3	14.0 ± 11.3
	D	0	0	$1.5 \times 10^4 \pm 3.7 \times 10^4$	0	0	$1.9 \times 10^4 \pm 4.2 \times 10^4$	$2.4 \times 10^2 \pm 7.1 \times 10^2$
	B	0	0	$2.1 \times 10^7 \pm 5.3 \times 10^7$	0	0	$2.8 \times 10^7 \pm 6.0 \times 10^7$	$3.4 \times 10^5 \pm 1.0 \times 10^6$

Sampling sites were grouped in outer (S1–S3), intermediate (S4–S6) and inner (S7–S9) sites. A, autumn; W, winter; Sp, spring; Su, summer.

and biovolume correlated significantly to distance only during the warm seasons (Table III). The total biovolume and PCA1 only correlated significantly in spring.

When considering the size-abundance spectra along the distance and elevation gradient, a decrease in the density of larger cells (>20 μm) was observed from S1 to S9, with smaller cells (2–5 μm ESD) remaining invariant (Fig. 4). Larger unicellular plankton (>10 μm ESD), however, accounted for the main contribution to the relative total biovolume during most of the year (Fig. 5) except in spring, when sites 7–9 showed particularly high densities of nanoplanktonic organisms (10–20 μm ESD).

The log–log analyses between total density and individual cell biovolume (by applying both OLS and RMA regressions) provided a good description of the size structure of unicellular plankton along the environmental gradient for each season. Most regressions for each site and season were significant, with slopes ranging from −0.78 to −0.14 for OLS and from −1.15 to −0.33 for RMA (Supplementary data, Table SI). The relative importance of larger phytoplankton in terms of its contribution to total biovolume decreased significantly toward inner waters in all seasons (using distance, elevation and PCA1 as dependent variables; Table IV). However, although Spearman coefficients were greater than 0.6 (in magnitude), RMA slopes did not correlate significantly with any of these variables in winter.

As shown in Fig. 6 and Table II, diatoms and small flagellates were the most abundant organisms among the 5 groups considered, accounting altogether for over 75%

Table III: Spearman correlation analysis among phytoplankton density and biovolume and spatial/environmental variables: distance, elevation and axis 1 of PCA (PCA1) based on environmental variables

Winter	Density	Biovolume	PCA1	Elevation	Distance
Density	1	0.81	0.03*	0.1	0.12
Biovolume	−0.08	1	0.11	0.05*	0.11
PCA1	0.75	−0.57	1	<0.001*	0.02*
Elevation	0.58	−0.66	0.9	1	<0.001*
Distance	0.55	−0.57	0.83	0.88	1
Spring	Abundance	Biovolume	PCA1	Elevation	Distance
Density	1	0.01*	0.01*	<0.001*	0.04*
Biovolume	0.98	1	0.01*	<0.001*	0.04*
PCA1	0.93	0.92	1	<0.001*	0.02*
Elevation	0.9	0.9	0.95	1	<0.001*
Distance	0.73	0.72	0.8	0.88	1
Summer	Abundance	Biovolume	PCA1	Elevation	Distance
Density	1	0.03*	0.04*	<0.001*	0.01*
Biovolume	0.75	1	0.51	0.01*	0.05*
PCA1	0.73	0.23	1	0.06	0.05*
Elevation	0.96	0.79	0.65	1	<0.001*
Distance	0.93	0.7	0.7	0.88	1
Autumn	Abundance	Biovolume	PCA1	Elevation	Distance
Density	1	0.48	0.05*	0.48	0.6
Biovolume	0.29	1	0.66	0.29	0.43
PCA1	0.79	−0.18	1	0.12	0.1
Elevation	0.29	−0.43	0.64	1	0.07
Distance	0.21	−0.32	0.68	0.75	1

Below diagonal are Spearman correlations coefficients, above diagonal are *P*-valued. * indicates significative correlations.

of the total density in almost all sites and seasons. Total ciliates (loricate and non-loricate) and larger flagellates declined toward the inner sites of the bay (31 and 26% of decline in density, respectively). Dinoflagellates, mainly represented by *Ceratium tripos*, *Ceratium inflatus*, *Triceratium favus* and *Protoperidinium* spp., showed small densities throughout the year in all sites, with their maximum contribution to total density outside the bay and channel (S1, S2 and S3) in winter (maximum 9.5%). Mainly in spring, and to a lesser extent in summer, high densities (mean, 1.9×10^4 ind.mL^{-1} and 2.4×10^2 ind.mL^{-1}, respectively) of meroplanktonic stages (gametes and zoospores) of the macroalgae *Ulva lactuca* were registered in the inner sites of the bay, representing over 95% of all planktonic cells. The spatial distribution of diatoms showed a pronounced ESD decrease from the outer SMG to the inner SAB waters (Fig. 7). The same trend was also followed by diatom total densities, where differences of one order of magnitude were observed between SMG and the internal channels (Mx. 2 235 cell. L^{-1} at S8). Most of the diatom taxa found in SAB were of benthic origin. Two of them, the naviculoides complex (sole representative of the 2–5 μm ESD range) and *Cylindrotheca closterium* (5–10 μm ESD), occurred in 100% of the samples, with highest densities (mean, $\sim 8 \times 10^2$ ind.mL^{-1}) at sites 7–9. These taxa were followed by *Grammatophora marina* and *Cocconeis* spp., though in much lower densities. Larger size diatoms found in outer waters (*Odontella* spp., > 80 μm; *Chaetoceros constrictus*, > 80 μm; *Thalassiosira* spp., 20–40 μm; *Thalassionema nitzschioides*, 10–20 μm; *Rhizosolenia styliformis*, 10–20 μm) were mostly of planktonic origin and were present in low densities. The full taxonomic lists and abundance data of diatoms and dinoflagellates are available as supplementary data (Table SII).

The PCA conducted with both species abundances (Fig. 8) and species biovolume (figure not presented) showed the same ordination of sites, where the first two axis accounted for 42.6% of the variance (for species abundances) and 42.4% (for species biovolume). In line with the above description, sites located outside the bay and channel (S1, S2 and S3) were positively associated to dinoflagellates and large-sized phytoplankton species and differed from intermediate sites (S4, S5 and S6), which where associated to smaller, typical coastal species. Inner sites (S7, S8 and S9) were positively associated to small groups of phytoplankton.

DISCUSSION

SAB shows a strong variation in its physical, chemical and biological properties from SMG to the inner channels, as the elevation of land increases. Like other Patagonian bays, SAB is protected from ocean waves because the prevailing winds are from the west (Isla *et al.*, 2001). Tides, therefore, are the main driver of the morphodynamic processes in this area, shaping it to a convex-up bottom profile previously described by Bearman *et al.* (2010) and involving a number of landward features such as high

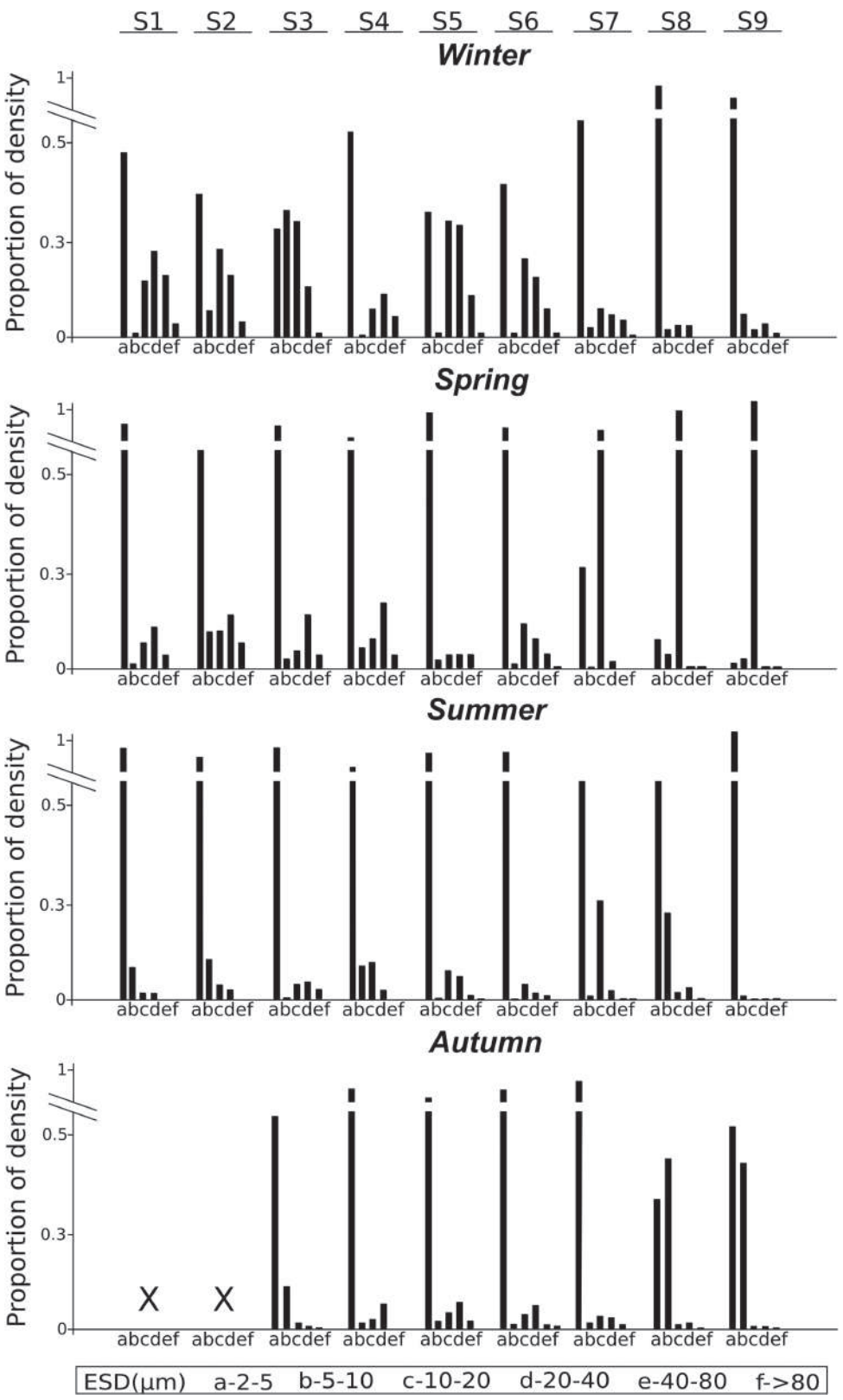

Fig. 4. Spatial and seasonal distribution of the density proportion of eukaryotic unicellular plankton size classes (a–f) based on the ESD in SAB. Sites (S1–S9) were sorted from outer (left) to inner waters (right). X, no samples available.

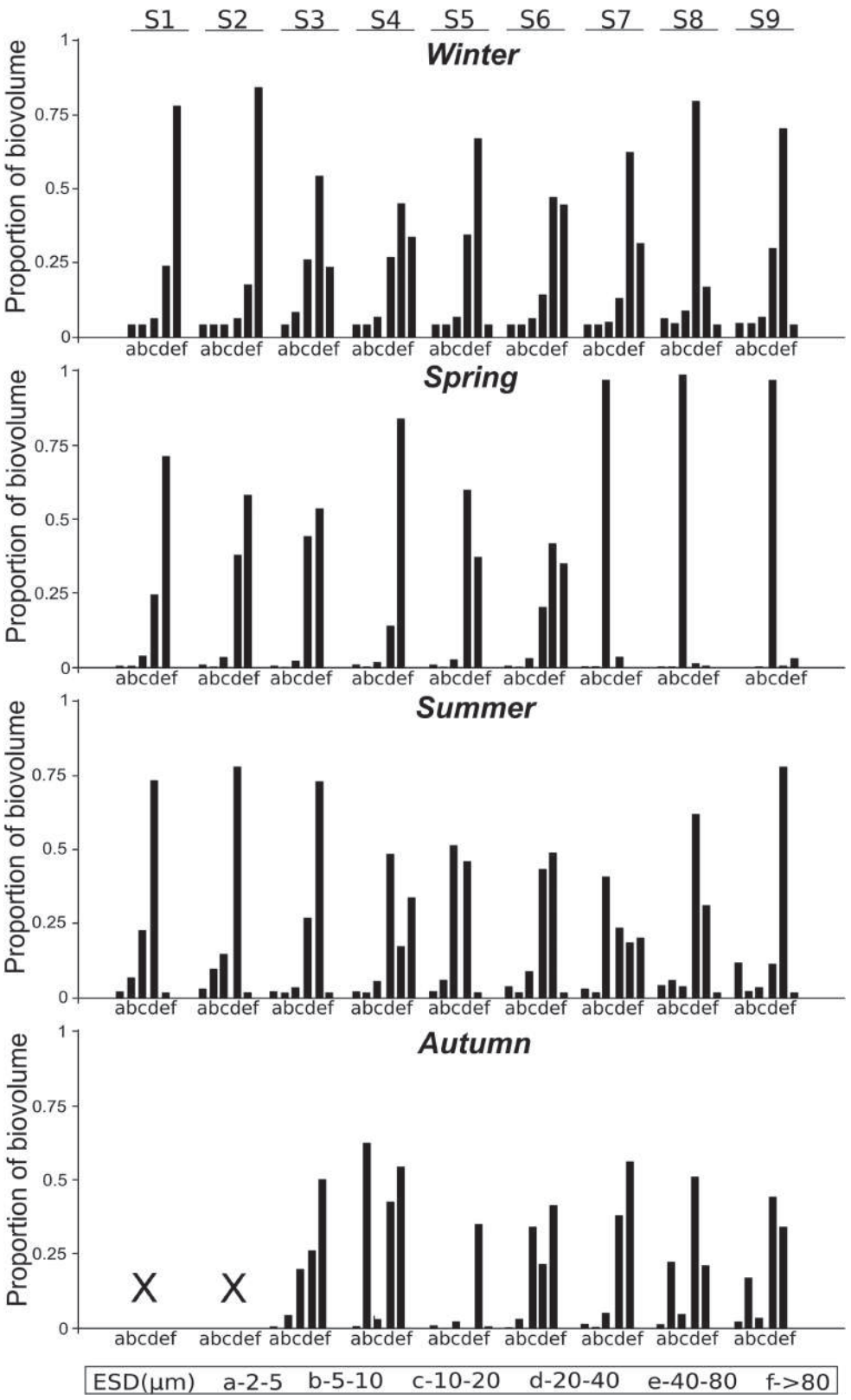

Fig. 5. Spatial and seasonal distribution of the biovolume proportion of eukaryotic unicellular plankton size classes (a–f) based on the ESD in SAB. Sites (S1–S9) were sorted from outer (left) to inner waters (right). X, no samples available.

Table IV: Spearman correlation analysis of eukaryotic unicellular plankton size spectrum: slopes of log–log regression analysis using both OLS and reduced major analysis (RMA) methods vs. distance, elevation, and axis 1 of PCA (PCA1) based on environmental variables

Winter	Slope log–log(OLS)	Slope log–log(RMA)	PCA1	Elevation	Distance
Slope log–log (OLS)	1	0.06	0.01*	0.01*	0.02*
Slope log–log (RMA)	0.67	1	0.06	0.08	0.07
PCA1	−0.87	−0.67	1	<0.001*	0.02*
Elevation	−0.81	−0.61	0.9	1	<0.001*
Distance	−0.83	.0,63	0.83	0.88	1
Spring	Slope log–log (OLS)	Slope log–log(RMA)	PCA1	Elevation	Distance
Slope log–log (OLS)	1	0.03*	0.01*	<0.001*	0.01*
Slope log–log (RMA)	0.75	1	0.05*	0.02*	0.07
PCA1	−0.88	−0.70	1	<0.001*	0.02*
Elevation	−0.95	−0.74	0.95	1	<0.001*
Distance	−0.92	−0.63	0.8	0.88	1
Summer	Slope log–log (OLS)	Slope log–log(RMA)	PCA1	Elevation	Distance
Slope log–log (OLS)	1	<0.001*	0.05*	0.04*	0.06
Slope log–log (RMA)	0.98	1	0.03*	0.02*	0.02*
PCA1	−0.68	−0.71	1	0.06	0.05*
Elevation	−0.69	−0.74	0.65	1	<0.001*
Distance	−0.67	−0.75	0.7	0.88	1
Autumn	Slope log–log (OLS)	Slope log–log(RMA)	PCA1	Elevation	Distance
Slope log–log (OLS)	1	0.02*	0.04*	0.08	0.07
Slope log–log (RMA)	0.83	1	0.02*	0.14	0.12
PCA1	−0.77	−0.96	1	0.12	0.1
Elevation	−0.7	−0.61	0.64	1	0.07
Distance	−0.72	−0.64	0.68	0.75	1

For each season, upper right figures indicate Spearman correlation coefficients while lower left figures indicate *P*-values. Asterisks specify significant correlations.

sediment transport, increased deposition, decreased grain size, a prograding profile and a locally shortened high water slack (Friedrichs, 2011).

The environmental gradient described in the present study is similar to the typical patterns found in other coastal environments like estuaries, where variables such as temperature, Chl-*a*, nutrients and CDOM increase from outer marine waters to the inner channels (Morais *et al.*, 2016; Guinder *et al.*, 2012). Sr values fell within the range observed for the Delaware estuary by Helms *et al.* (2008) and were found to decrease from outer marine waters to SAB inner channels. Higher values may be indicating low molecular weight material or decreasing aromaticity. In contrast, lower values (S7–S9) may represent a mixing process with wastewater or fresh water that incorporates absorbing substances or that could be produced by microbial activity (Helms *et al.*, *op. cit.*).

However, an opposite trend for salinity was found. Given its location in an arid region with no river input or stream discharge, evaporation of interstitial water is enhanced in inner channels as sediments remain uncovered for a prolonged period of time (Wang *et al.*, 2007), thus promoting an increase in salinity values as entering the bay.

Some of the environmental variables changed in accordance with the strong seasonality of the area. The landward pattern of decreasing temperatures in winter and increasing temperatures in summer responds to the pronounced heat exchange that takes place due to the shallowness of the system. In line with this temperature pattern, salinity was also observed to increase during the warm seasons due to enhanced evaporation. Chl-*a* values also varied seasonally and were higher during spring and, to a lesser extent, in summer, when nutrient availability and temperature provide an enabling environment for the growth of phytoplankton.

The tidal effect in SAB exerts a gradual sorting effect on larger eukaryotic unicellular plankton due to the sedimentation of larger groups as the water mass loses energy, thus resulting in the decrease of total biovolume landwards in autumn and winter. These dynamics match those of the conceptual convex-up model (Friedrichs, 2011), which explains the behavior of flats for high tidal ranges and decreasing wave action, where the landward decrease in water depth results in a reduction of current velocity thus promoting the sedimentation of suspended matter and, consequently, a smaller sediment and plankton load in the water column. At the same time, the remaining small-cell populations with high intrinsic growing rate find proper environmental conditions to replicate in less turbulent areas (inner sites of the SAB), which explains the increase of total density landwards along the year. In this line, Legendre *et al.* (1982) and Walsh (1981) registered phytoplankton blooms in stable water columns after days

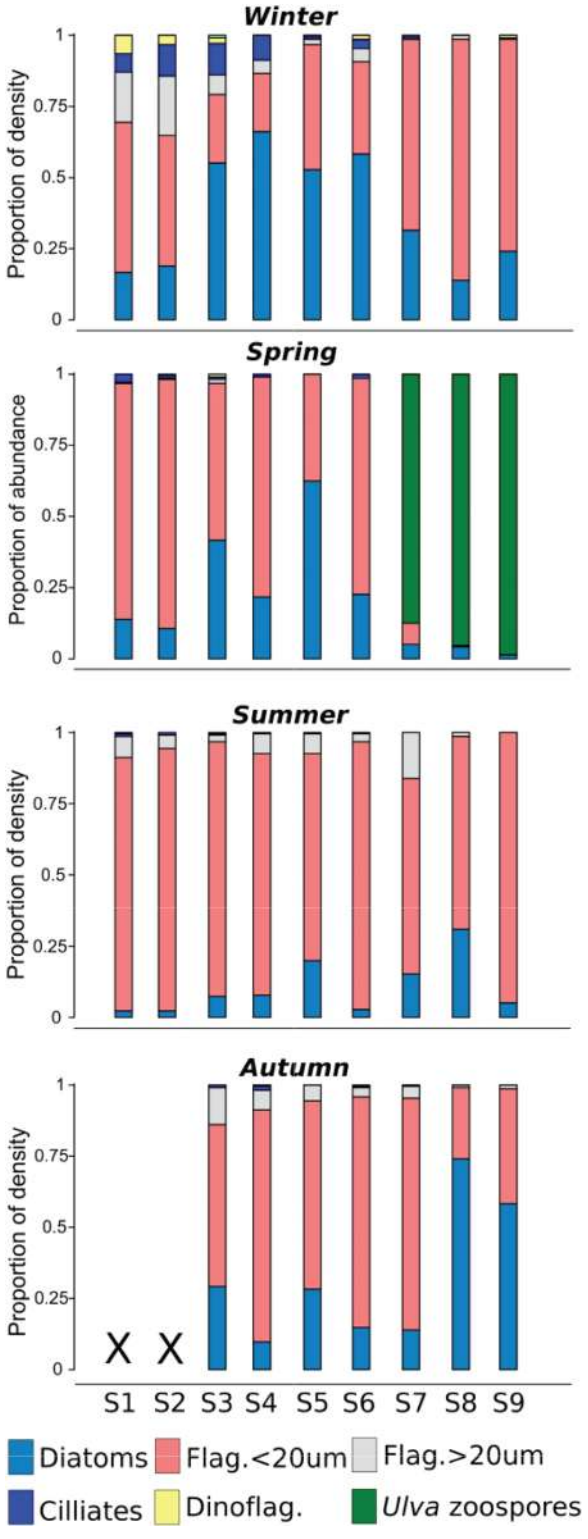

Fig. 6. Relative density of the main eukaryotic unicellular planktonic groups recorded in SAB at each sampling site in each season of the year. Sites (S1–S9) were sorted from outer (left) to inner waters (right). X, no samples available.

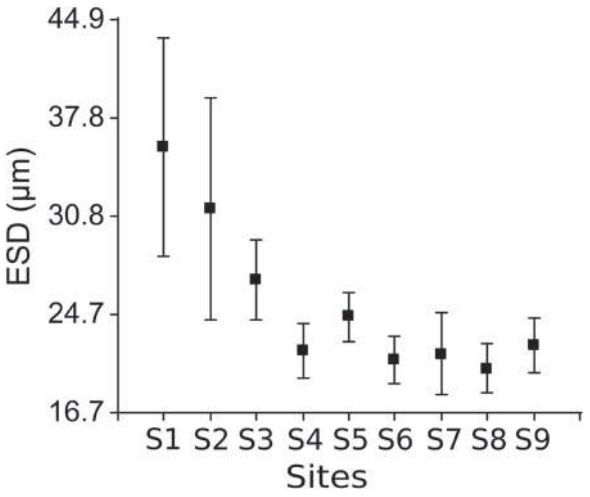

Fig. 7. Spatial variation of the ESD of diatoms at each sampling site in SAB. Sites (S1–S9) were sorted from outer (left) to inner waters (right). Each point represents the yearly mean ESD value; bars represent the standard error.

of wind stress. Moreover, in environments with low turbulent mixing, the proliferation of phytoplankton patches induced by local conditions was observed in contrast to well-mixed areas (Therriault and Platt, 1981). The passive retention of particles in high estuaries only by tidal action has been previously described by Morgan *et al.* (1997) and may explain the increase of phytoplankton density landward across the flat in SAB. Additionally, the inner sites in SAB presented proportionally higher cell sizes in warmer seasons than in colder ones, which suggests that other factors such as resource availability and/or light limitation (rather than temperature) are often responsible for the presence of larger plankton cell sizes (Sommer *et al.*, 2017 and references therein). As compared to small cells, large cells are able to better evade microzooplankton grazing and can display higher photosynthetic efficiency and growing rates under non-limiting nutrient and light conditions (Cermeño *et al.*, 2005 and references therein), thus explaining their success in coastal environments (Cloern, 2018) and oceanic upwelling systems (Dugdale and Wilkerson, 1998). Accordingly, planktonic cells of higher size within SAB were found to be the main contributors to total plankton biovolume. Slope values from the log–log analysis ranged from −0.78 to −0.14 (mean, −0.43) for OLS regressions and from −1.15 to −0.33 (mean, −0.64) for RMA regressions, in line with those observed in assemblages of highly productive inshore waters (Huete-Ortega *et al.*, 2010; Reul *et al.*, 2005, 2008). Although both types of regression describe the same spatial pattern, slopes from OLS regressions were in all cases lower than RMA, a fact also verified by Laws and Archie (1981) when reanalyzing with RMA two ecological data sets previously

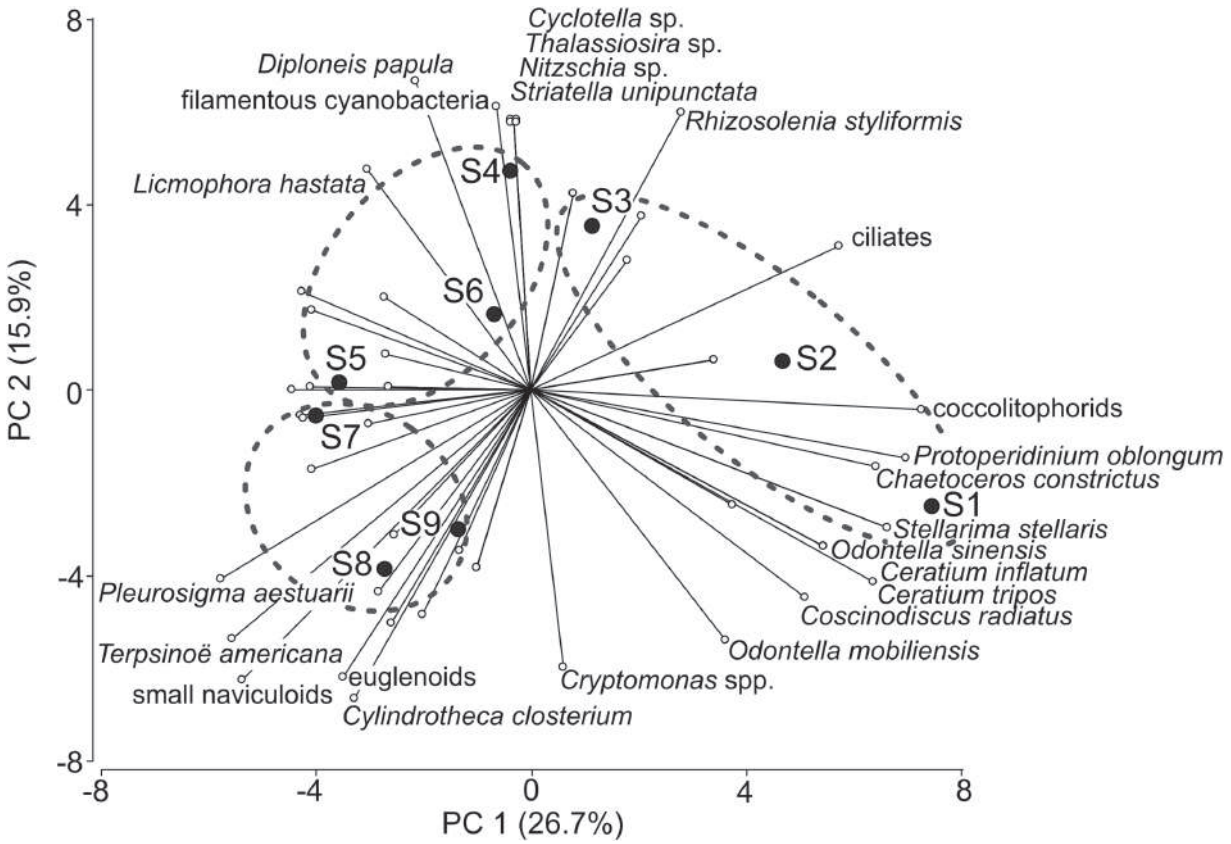

Fig. 8. Biplot of the PCA based on eukaryotic unicellular plankton abundances from nine sites at SAB (S1–S9). Rows indicate the loading of each species on the first two axes. Named species correspond to those earning a score higher than 0.2 for axis 1 or 2. Percentages on each axis indicate the amount of variance explained.

analyzed with OLS. As RMA regressions also include errors in the *x*-axis, it adds measurement errors to the inherent variability of the explanatory variable (Legendre and Legendre, 1998), thus proving to be the most appropriate method to describe the functional relationship between these variables. RMA regressions seem to be more appropriate for the analysis of plankton size spectra in particular (e.g. Huete-Ortega *et al.*, 2012; Marañón, 2014) and for trait-based approaches to community structure studies in general (e.g. López-Urrutia *et al.*, 2006; Litchman *et al.*, 2007).

Differences among planktonic size spectra across the studied area evidence a general decreasing contribution of larger size phytoplankton to total biovolume toward the inner sites in the bay, a pattern that was held throughout the year. Two aspects should be stressed to this respect. In the first place, and taking into account that the aim of this study is not a characterization of species richness and diversity, large-size species are generally rare and commonly present in low numbers within phytoplanktonic communities (Rodríguez-Ramos *et al.*, 2014; Cermeño *et al.*, 2014). The recommended sample volume to be analyzed for the detection of 90% of the species is from 0.25 to 1 L, depending on the concentration of phytoplankton (Cermeño *et al.*, *op. cit.*). Although the sample size used in this study for quantitative processes was lower than that recommended and might therefore represent a source of error, it was always backed with the observation of net samples (15 μm net) in order to minimize the bias associated with the detection of large cells. In the second place, it is well known that the sinking rate of phytoplankton greatly depends on cell shape, buoyancy control and the presence of flagella (e.g. Padisàk *et al.*, 2003). However, cell size is also mentioned as a key feature for phytoplankton sinking (Marañón, 2009), with larger cells exhibiting a higher sinking rate than smaller ones (Takahashi and Bienfang, 1983). During the SAB tidal cycle, the incoming mass of water decreases its strength landwards so suspended particles (including planktonic cells) show a sinking gradient in accordance with their size: while larger fractions tend to sink in outer waters, smaller ones can remain suspended even at the shoreline.

A comparison of the present results with those reported by Santinelli *et al.* (2018) for different Patagonian coastal environments (including two sites close to SAB) reveals that the total mean abundance registered in SAB and surrounding areas (8.0×10^3 ind.mL^{-1}) is positioned in the upper end for the densities reported ($\sim 10^3$ ind.mL^{-1} in Nueva Bay, Engaño Bay, Golondrina Bay and the Deseado Estuary). Phytoplankton assemblages were found to join together organisms distinctive of coastal, eutrophic environments with others typically oceanic. Additionally, the mean total abundance and planktonic community structure recorded at the outer sites (S1, S2 and S3) are in line with those found by Hoffmeyer *et al.* (*op. cit.*) near the boundaries of SAB.

Due to their broad size range and high abundance, diatoms accounted for the bulk of size variation observed toward shallower coastal sites. Previous studies in SAB (Esteves *et al.*, 1996) and on other Argentine coastal environments such as the Bahía Blanca estuary (Gayoso, 1998; Guinder *et al.*, 2009) and Bahía Engaño (Villafañe *et al.*, 2004) agree in remarking the dominance of diatoms, thus suggesting that this might be a feature common to all northern Patagonian locations. Also flagellates were dominant in SAB in terms of density, for almost all sites and seasons; however, they did not contribute to the bulk of the total plankton biovolume. Despite flagellated cells are of great importance for primary production and picoplankton grazing in the open ocean (Massana and Pedrós-Alió, 2008), in nutrient rich systems larger phytoplankton cells tends to overcome in biomass (Cloern, 2018). Dinoflagellates, in turn, were present in low densities and mainly in SMG, in agreement with Sastre *et al.* (1995) who found relatively higher densities of dinoflagellates in waters of the same area. According to Carreto *et al.* (1974), SMG presents two clearly distinct zones: a northeastern sector (adjacent to SAB) dominated by dinoflagellates and characterized by higher temperature and salinity, a marked thermocline and limiting concentrations of nitrates and a southeastern sector dominated by diatoms, with lower temperature and salinity, null stratification and relatively higher concentrations of nitrates. In fact a seasonal front system was described for the area and the two water masses better spatially defined (Gagliardini and Rivas, 2004; Williams *et al.*, 2013). In this context, the seminal trait-based "mandala" model proposed by Margalef (1978) and Margalef *et al.* (1979) frames our results, as it relates the phytoplankton functional morphology to adaptive strategies in response to disturbance (i.e. turbulence) and nutrient content: this model makes the distinction between organisms such as diatoms, which develop under turbulent and high-nutrient conditions, and those such as dinoflagellates, which thrive in nutrient-poor and low turbulence environments.

Given the high levels of phosphates and nitrates in SAB, higher Chl-*a* values were expected. Nevertheless, the Chl-*a* concentration range was from moderate to low (0.5–12.4 mg.m^{-3}) and much lower as compared to other Patagonian bays like Bahía Engaño (up to 100 mg.m^{-3}; Villafañe *et al.*, 2004) and the Bahía Blanca estuary (up to 40.2 mg.m^{-3}; Spetter *et al.*, 2015). We hypothesize that SAB's ample tidal range might prevent high biomass accumulation, as observed for other coastal systems (Bonilla *et al.*, 2005). This process can be framed within the "outwelling hypothesis" (Odum, 1968, 2002), by which coastal environments with high tidal amplitudes would be net providers of nutrients, organic matter and organisms to surrounding areas, thus sustaining secondary production. This likely mechanism is also supported by the fact that the number of diatom taxa (mostly of benthic origin) recorded in SAB was higher than that of SMG (for the most part typically planktonic). Additionally, the nutrient-Chl-*a* decoupling observed can also be explained by the significant grazing pressure commonly exerted on coastal phytoplankton by intertidal filtering animals (Lonslade *et al.*, 2009), zooplankton (Bautista and Harris, 1992) and microheterotrophs (Nixon *et al.*, 1986).

The input of nutrients and organic matter in SAB, increased by human activities, may be masked by the large amount of water circulating during each tidal cycle (Martinetto *et al.*, 2010). Moreover, nutrients and biological products seem to be concentrated during low tide and diluted with every high tide (Martinetto *et al.*, 2010). However, the high densities of unicellular plankton (and particularly of meroplanktonic stages of *U. lactuca*) found in shallow waters of the bay suggest that the washout does not have a significant impact on the inner channels. Triggered by the large land-derived nutrient input, particularly dissolved inorganic nitrogen (Teichberg *et al.*, 2010), *U. lactuca* is known to produce green tides in SAB channels during springtime (Gastaldi *et al.*, 2016), which support high densities of consumers by increasing food availability (Martinetto *et al.*, 2010).

Likewise, some phytoplanktonic species (e.g. *C. closterium*, *Leptocylindrus minimus*, *Pseudonitzchia* sp. and euglenoids) often linked to high-nutrient concentration and the impoverishment of water quality (e.g. Jaanus *et al.*, 2009; Parsons *et al.*, 2002), and therefore used as bioindicators (Parmar *et al.*, 2016), were also detected in the SAB inner channels. As well, some of the so-called harmful species found in our study were previously reported by Sunensen *et al.* (2009) from the surroundings of SAB. Despite none of them were found to cause detectable harmful effects, their presence should be taken as a warning and motivate a comprehensive monitoring of water quality.

CONCLUSION

In this study, we provide the first outlook of the planktonic assemblages of SAB and the environmental variables that might govern them. Although higher contributions to total biovolume lie on groups of relatively larger size, we found these to decrease in importance landwards across the flat, defining a pattern that is held through seasons. These results provide evidence of the importance of tides on the taxonomic and size structure of lower trophic levels of the food web in temperate tidal flats under strong macrotidal regimes, as well as the relevance of local factors triggering the density increase of certain taxa (*U. lactuca*, dinoflagellates). Future studies at SAB will have to explore the spatial and seasonal trends during high tide and also to what extent the phototrophs (phytoplankton, macroalgae and microphytobenthos) compete for light, nutrients and inorganic carbon.

ACKNOWLEDGEMENTS

Authors thank the valuable comments and suggestions made by reviewers that greatly improve the manuscript. Support provided by the staff of Escuela Superior de Ciencias Marinas and Centro de Investigación Aplicada y Transferencia Tecnológica en Recursos Marinos Almirante Storni is gratefully acknowledged.

FUNDING

Agencia Nacional de Investigación Científica y Tecnológica; Instituto Antártico Argentino (PICT-O 0128 to V.A.A., PICT 2017-4374 to J.F.S); Postdoctoral Fellowship of Consejo Nacional de Investigaciones Científicas y Técnicas (J.F.S.).

REFERENCES

Acevedo-Trejos, E., Brandt, G., Merico, A. and Smith, S. L. (2013) Biogeographical patterns of phytoplankton community size structure in the oceans. *Glob. Ecol. Biogeogr.*, **22**, 1060–1070 https://doi.org/10.1111/geb.12071.

Alder, V. A. and Morales, C. (2009) *Manual de Métodos para el Estudio de los Sistemas Planctónicos Marinos*, EUDEBA, Buenos Aires, p. 267.

[APHA] American Public Health Association (2012) *Standard Methods for the Examination of Water and Wastewater*, 22nd edn, Washington.

Balech, E. (1988) *Los Dinoflagelados del Atlántico Sudoccidental*. Publicaciones especiales, Instituto Español de Oceanografía, Madrid, 310pp.

Bautista, B. and Harris, R. P. (1992) Copepod gut contents, ingestion rates and grazing impact on phytoplankton in relation to size structure of zooplankton and phytoplankton during a spring bloom. *Mar. Ecol. Prog. Ser.*, **82**, 41–50 https://doi.org/10.3354/meps082041.

Bearman, J. A., Driedrichs, C. T., Jaffe, B. E. and Jaffe, B. E. (2010) Spatial trends in tidal flat shape and associated environmental parameters in South San Francisco Bay. *J. Coast. Res.*, **262**, 342–349 http://dx.doi.org/10.2112/08-1094.1.

Boltovskoy, D. (1981) *Atlas del Zooplancton del Atlántico Sudoccidental y Métodos de Trabajo con el Zooplancton Marino*, Publicación Especial del INIDEP, Mar de Plata, p. 936.

Bonilla, S., Conde, D., Aubriot, L. and Pérez, C. (2005) Influence of hydrology on phytoplankton species composition and life strategies in a subtropical coastal lagoon periodically connected with the Atlantic Ocean. *Estuaries*, **28**, 884–895 https://doi.org/10.3354/meps293155.

Carbone, M. E., Perillo, G. M. E. and Piccolo, M. C. (2007) Dinámica morfológica de los ambientes costeros de la bahía San Antonio, provincia de Río Negro. *Geoacta*, **32**, 83–91.

Carreto, J. I., Verona, C. A., Casal, A. B. and Laborde, M. A. (1974) Fitoplancton, pigmentos y condiciones ecológicas del Golfo San Matías III. Inst. Biol. Mar. Mar del Plata, Contr. 237. Informe 10 de la Comisión de Investigaciones Científicas de la Provincia de Buenos Aires, pp. 49–76.

Cermeño, P., Marañón, E., Rodriguez, J. and Fernandez, E. (2005) Large-sized phytoplankton sustain higher carbon-specific photosynthesis than smaller cells in a coastal eutrophic ecosystem. *Mar. Ecol. Prog. Ser.*, **297**, 61–60.

Cermeño, P., Texeira, I. G., Blanco, M., Figueiras, F. G. and Marañón, E. (2014) Sampling the limits of species richness in marine phytoplankton communities. *J. Plankton Res.*, **36**, 1135–1139 https://doi.org/10.1093/plankt/fbu033.

Cicchetti, G. and Diaz, R. J. (2002) Types of salt marsh edge and export of trophic energy from marshes to deeper habitats. In Weinstein, M. P. and Kreeger, D. A. (eds.), *Concepts and Controversies in Tidal Marsh Ecology*, Springer, Netherlands, pp. 515–541.

Cloern, J. E. (2018) Why large cells dominate estuarine phytoplankton. *Limnol. Oceanogr.*, **63**, S392–S409 https://doi.org/10.1002/lno.10749.

Dugdale, R. C. and Wilkerson, F. P. (1998) Silicate regulation of new production in the equatorial Pacific upwelling. *Nature*, **391**, 270–273 https://doi.org/10.1038/34630.

Esteves, J., Solís, M., Sastre, V., Santinelli, M., Gil, M., Commendatore, M. and Raies, C. G. (1996) Evaluación de la contaminación urbana de la bahía de San Antonio (Provincia de Río Negro). Informes técnicos del Plan de Manejo de la Zona Costera Patagónica, Fundación Patagonia Natural, Puerto Madryn, Argentina.

Friedrichs, C. T. (2011) Tidal flat morphodynamics: a synthesis. In Flemming, B. W. and Hanson, M. D. (eds.), *Treatise on estuarine and coastal science, sedimentology and geology*, Elsevier, pp. 137–170 https://doi.org/10.1016/B978-0-12-374711-2.00307-7.

Gagliardini, D. A. and Rivas, A. L. (2004) Environmental characteristics of San Matías gulf obtained from landsat-TM and ETM+ data. *Gayana*, **68**, 186–193.

Gastaldi, M., Firstater, F. N., Daleo, P. and Narvarte, M. A. (2016) Abundance of the sponge *Hymeniacidon* cf. *perlevis* in a stressful environment of Patagonia: relationships with *Ulva lactuca* and physical variables. *J. Mar. Biol. Assoc. U. K.*, **96**, 465–472 http://dx.doi.org/10.1017/S0025315415001198.

Gayoso, A. M. (1998) Long-term phytoplankton studies in the Bahía Blanca Estuary, Argentina. *ICES J. Mar. Sci.*, **55**, 655–660 https://doi.org/10.1006/jmsc.1998.0375.

Guinder, V. A., Popovich, C. A. and Perillo, G. M. E. (2009) Short-term variability in the phytoplankton and physico-chemical variables in a high-tidal regime, Bahía Blanca Estuary, Argentina. *Braz. J. Oceanogr.*, **57**, 249–258 https://doi.org/10.1590/S1679-87592009000300008.

Guinder, V. A., Popovich, C. A. and Perillo, G. M. E. (2012) Phytoplankton and physicochemical analysis on the water system of the temperate estuary in South America: Bahía Blanca Estuary, Argentina. *Int. J. Environ. Res.*, **6**, 547–556 http://ijer.ut.ac.ir/images/Issues/Vol6.No2/22.rar.

Hansen, A. M., Kraus, T. E. C., Pellerin, B. A., Fleck, J. A., Downing, B. D. and Bergamaschi, B. A. (2016) Optical properties of dissolved organic matter (DOM): effects of biological and photolytic degradation. *Limnol. Oceanogr.*, **61**, 1015–1032 https://doi.org/10.1002/lno.10270.

Hayes, M. O. (1979) Barrier island morphology as a function of tidal and wave regime. In Leatherman, S. P. (ed.), *Barrier Islands from the Gulf of St. Lawrence to the Gulf of Mexico*, Academic Press, New York, pp. 1–27.

Helms, J. R., Stubbins, A., Ritchie, J. D., Minor, E. C., Kieber, D. J. and Mopper, K. (2008) Absorption spectral slopes and slope ratios as indicators of molecular weight, source, and photobleaching of chromophoric dissolved organic matter. *Limnol. Oceanogr.*, **53**, 955–969.

Hillebrand, H., Claus-Dieter, D., Kirschtel, D., Pollingher, U. and Zohary, T. (1999) Biovolume calculation for pelagic and benthic microalgae. *J. Phycol.*, **35**, 403–424 https://doi.org/10.1046/j.1529-8817.1999.3520403.x.

Hinde, H. P. (1954) The vertical distribution of salt marsh phanerogams in relation to tide levels. *Ecol. Monogr.*, **24**, 209–225 https://www.doi.org/10.2307/1948621.

Huete-Ortega, M., Marañón, E., Varela, M. and Bode, A. (2010) General patterns in the size scaling of phytoplankton abundance in coastal waters during a 10-year time series. *J. Plankton Res.*, **32**, 1–14 https://doi.org/10.1093/plankt/fbp104.

Huete-Ortega, M., Cermeõo, P., Calvo-Díaz, A. and Marañón, E. (2012) Isometric size-scaling of metabolic rate and the size abundance distribution of phytoplankton. *Proc. R. Soc. B.*, 279: 1815–1823.

Ibañez, C., Curcó, A., Day, J. W. D. and Prat, N. (2000) Structure and productivity of microtidal Mediterranean coastal marshes. In Weinstein, M. and Kreeger, D. A. (eds.), *Concepts and Controversies in Tidal Marsh Ecology*, Kluwer Academic Publishing, pp. 107–136.

Isla, F. I., Bértola, G. I. and Schnack, E. J. (2001) Morfodinámica de playas meso y macromareales de Buenos Aires, Río Negro y Chubut. *Rev. Asoc. Argen. Sedimentol.*, 8:51–60.

Jaanus, A., Toming, K. and Hällfors, S. (2009) Potential phytoplankton indicator species for monitoring Baltic coastal waters in the summer period. *Hydrobiologia*, **629**, 157–168.

Koch, F. and Gobler, C. J. (2009) The effects of tidal export from salt marsh ditches on estuarine water quality and plankton communities. *Estuaries Coasts*, **32**, 261–275 https://doi.org/10.1007/s12237-008-9123-y.

Kwak, T. J. and Zedler, J. B. (1997) Food web analysis of southern California coastal wetlands using multiple stable isotopes. *Oecologia*, **110**, 262–277 https://doi.org/10.1007/s004420050159.

Laws, E. and Archie, J. W. (1981) Appropriate use of regression analysis in marine biology. *Mar. Biol.*, **65**, 13–16.

Legendre, L., Ingram, R. G. and Simard, Y. (1982) Aperiodic changes of water column stability and phytoplankton in an Arctic coastal embayment, Manitounuk Sound, Hudson Bay. *Nat. Can.*, **109**, 775–786.

Legendre, P. and Legendre, L. (1998) *Numerical Ecology*, 2nd. edn, Elsevier Science, Amsterdam, p. 852.

Litchman, H., Klausmeier, C. A., Schofield, O. M. and Falkowski, O. M. (2007) The role of functional traits and trade-offs in structuring phytoplankton communities: scaling from cellular to ecosystem level. *Ecol. Lett.*, **10**, 1170–1181.

Lorenzen, C. J. (1967) Determination of chlorophyll and pheopigments: spectrophotometric equations. *Limnol. Oceanogr.*, **12**, 343–346 https://doi.org/10.4319/lo.1967.12.2.0343.

Lonslade, D. J., Carreto, R. M., Holland, R., Mass, A., Holt, L., Schaffner, R. A., Pan, J. and Caron D. A. (2009) Influence of suspension-feeding bivalves on the pelagic food webs of shallow, coastal embayments. *Aquat. Biol.*, **6**, 263–279 https://www.doi.org/10.3354/ab00130.

López-Urrutia, A., San Martin, E., Harris, R. P. and Irigoien, X. (2006) Scaling the metabolic balance of the oceans. *Proc. Natl. Acad. Sci. U. S. A.*, **103**, 8739–8744.

Margalef, R. (1978) Life-forms of phytoplankton as survival alternatives in an unstable environment. *Oceanol. Acta*, **1**, 493–509.

Margalef, R., Estrada, M. and Blasco, D. (1979) Functional morphology of organisms involved in red tides, as adapted to decaying turbulence. In Taylor, D. and Selinger, H. (eds.), *Toxic Dinoflagellates Blooms*, Elsevier, New York, pp. 178–185.

Marañón, E. (2009) Phytoplankton size structure. In Steele, J. H., Turekian, K. K. and Thorpe, S. A. (eds.), *Encyclopedia of Ocean Sciences*, 2nd edn, Academic Press, Oxford, https://doi.org/10.1016/B978-012374473-9.00661-5.

Marañón, E. (2014) Cell size as a key determinant of phytoplankton metabolism and community structure. *Ann. Rev. Mar. Sci.*, **7**, 241–264.

Marker, A. F. H., Nusch, A., Rai, H. and Riemann, B. (1980) The measurement of photosynthetic pigments in freshwater and standardization of methods: conclusions and recommendations. *Arch. Hydrobiol. Beih. Ergebn. Limnol.*, **14**, 91–106.

Martinetto, P., Daleo, P., Escapa, M., Alberti, J., Isacch, J. P., Fanjul, E., Botto, F., Piriz, M. L., *et al.* (2010) High abundance and diversity of consumers associated with eutrophic areas in a semi-desert macrotidal coastal ecosystem in Patagonia, Argentina. *Estuar. Coast. Shelf Sci.*, **88**, 357–364 https://doi.org/10.1016/j.ecss.2010.04.012.

Massana, R. and Pedrós-Alió, C. (2008) Unveiling new microbial eukaryotes in the surface ocean. *Curr. Opin. Microbiol.*, **11**, 213–218 https://doi.org/10.1016/j.mib.2008.04.004.

McManus, M. A. and Woodson, C. B. (2012) Plankton distribution and ocean dispersal. *J. Exp. Biol.*, **215**, 1008–1016 https://doi.org/10.1242/jeb.059014.

Morais, G. C., Camargo, M. G. and Lana, P. (2016) Intertidal assemblage variation across a subtropical estuarine gradient: how good conceptual and empirical models are? *Estuar. Coast. Shelf Sci.*, **170**, 91–101 https://doi.org/10.1016/j.ecss.2015.12.020.

Morgan, C. A., Cordell, J. R. and Simenstad, C. A. (1997) Sink or swim? Copepod population maintenance in the Columbia River estuarine turbidity-maxima region. *Mar. Biol.*, **129**, 309–317 https://doi.org/10.1007/s002270050171.

Murray, N. J., Phinn, S. R., DeWitt, M., Ferrari, R., Johnston, R., Lyons, M. B., Clinton, N., Thau, D. *et al.* (2019) The global distribution and trajectory of tidal flats. *Nature*, **565**, 222–225 https://doi.org/10.1038/s41586-018-0805-8.

Negrin, V. L., Spetter, C. V., Asteasuain, R. O., Perillo, G. M. E. and Marcovecchio, J. E. (2011) Influence of flooding and vegetation on carbon, nitrogen, and phosphorus dynamics in the pore water of a

Spartina alterniflora salt marsh. *J. Environ. Sci.*, **23**, 212–221 https://doi.org/10.1016/S1001-0742(10)60395-6.

Nixon, S. W., Oviatt, C. A., Frithsen, J. and Sullivan, B. (1986) Nutrients and the productivity of estuarine and coastal marine ecosystems. *J. Limnol. Soc. Sth. Afr.*, **12**, 43–71. https://doi.org/10.1080/03779688.1986.9639398.

Odum, E. P. (1968) A research challenge: evaluating the productivity of coastal and estuarine water. In *Proceedings of the 2nd Sea Grant Congress*. University of RI, Kingston.

Odum, E. P. (1980) The status of three ecosvstem-level hypothesis regarding salt marsh estuaries: tidal subsidy, outwelling, and detritus-based food chain. In Kennedy, V. S. (ed.), *Estuarine Perspectives*, Elsevier, pp. 485–495.

Odum, E. P. (2002) Tidal marshes as outwelling/pulsing systems. In Weinstein, M. P. and Kreeger, D. A. (eds.), *Concepts and Controversies in Tidal Marsh Ecology*, Springer, Dordrecht.

Padisàk, J., Soróczki-Pintér, É. and Rezner, Z. (2003) Sinking properties of some phytoplankton shapes and the relation of from resistance to morphological diversity of plankton—an experimental study. *Hydrobiologia*, **500**, 243–257 https://www.doi.org/10.1023/A:1024613001147.

Parmar, T. K., Rawtani, D. and Agrawal, Y. K. (2016) Bioindicators: the natural indicator of environmental pollution. *Front. Life Sci.*, **9**, 110–118 https://www.doi.org/10.1080/21553769.2016.1162753.

Parsons, M. L., Dortch, Q. and Turner, R. E. (2002) Sedimentological evidence of an increase in *Pseudo-nitzschia* (Bacillariophyceae) abundance in response to coastal eutrophication. *Limnol. Oceanogr.*, **47**, 551–558.

Quintana, X. D., Comín, F. A. and Moreno-Amich, R. (2002) Biomass size-spectra in aquatic in shallow fluctuating Mediterranean salt marshes (Empòrda wetlands, NE Spain). *J. Plankton Res.*, **24**, 1149–1161.

Reul, A., Rodríguez, V., Jimenez-Gomez, F., Blanco, J. M., Bautista, B., Sarhan, T., Guerrero, F., Ruíz, J., *et al.* (2005) Variability in the spatio-temporal distribution and size-structure of phytoplankton across an upwelling area in the NW-Alboran Sea, (W-Mediterranean). *Cont. Shelf Res.*, **25**, 589–608 https://doi.org/10.5697/oc.54-2.255.

Reul, A., Rodriguez, J., Guerrero, F., Gonzalez, N., Vargas, J. M., Echevarría, F. *et al.* (2008) Distribution and size biomass structure of nanophytoplankton in the Strait of Gibraltar. *Aquat. Microb. Ecol.*, **52**, 253–262.

Rodríguez-Ramos, T., Dornelas, M., Marañón, E. and Cermeño, P. (2014) Conventional sampling methods severely underestimate phytoplankton species richness. *J. Plankton Res.*, **36**, 334–343 http://doi.org/10.1093/plankt/fbt115.

R Core Team (2016) R: Language and environment for statistical computing. Vienna, Austria.

Sanderson, E. W., Ustin, S. L. and Foin, T. C. (2000) The influence of tidal channels on the distribution of salt marsh plant species in Petaluma Marsh, CA, USA. *Plant Ecol.*, **146**, 29–41 https://doi:10.1023/A:1009882110988.

Santinelli, N. H., Sastre, A. V., Gil, M. N. and Esteves, J. L. (2018) Composition and structure of phytoplankton communities in coastal environments with anthropogenic disturbance (Patagonia, Argentina). In Hoffmeyer, M. S., Sabatini, M. E., Brandini, F. P., Calliari, D. L. and Santinelli, N. H. (eds.), *Plankton Ecology of the Southwestern Atlantic: From the Subtropical to the Subantartic Realm*, Springer, Switzerland, pp. 519–540.

Sar, E. (1996a) Flora diatomológica de Bahía San Antonio (Prov. de Río Negro, Argentina). O. Centrales I. *Rev. Mus. La Plata. Sec. Bot.*, **14**, 365–400.

Sar, E. (1996b) Flora diatomológica de Bahía San Antonio (Prov. de Río Negro, Argentina). O. Pennales I. *Rev. Mus. La Plata. Sec. Bot.*, **14**, 399–432.

Sastre, A. V., Santinelli, N. H. and Esteves, J. L. (1995) Fitoplancton del Golfo San Matías de tres campañas de muestreo. *Physis Secc. A*, **53**, 7–12.

Shimeta, J. and Sisson, J. D. (1999) Taxon-specific tidal resuspension of protists into the subtidal benthic boundary layer of a coastal embayment. *Mar. Ecol. Prog. Ser.*, **177**, 51–62 https://doi.org/10.3354/meps177051.

Sommer, U., Peter, K. H., Genitsaris, S. and Moustaka-Gouni, M. (2017) Do marine phytoplankton follow Bergmann's rule sensu latu? *Biol. Rev.*, **92**, 1011–1026 https://www.doi.org/10.1111/brv.12266.

Spetter, C. V., Popovich, C. A., Arias, A., Asteasuain, R. O., Freije, R. H. and Marcovecchio, J. E. (2015) Role of nutrients in phytoplaknton development during a winter bloom in a eutrophic South American Estuary (Bahía Blanca, Argentina). *J. Coast. Res.*, **31**, 76–87 https://doi.org/10.2112/JCOASTRES-D-12-00251.1.

Sun, J. and Liu, D. (2003) Geometric models for calculating cell biovolume and surface area for phytoplankton. *J. Plankton Res.*, **25**, 1331–1346 https://doi.org/10.1093/plankt/fbg096.

Sunensen, I., Bárcena, A. and Sar, E. A. (2009) Diatomeas potencialmente nocivas del Golfo San Matías (Argentina). *Rev. Biol. Mar. Oceanogr.*, **44**, 67–88.

Takahashi, M. and Bienfang, P. K. (1983) Size structure of phytoplankton biomass and photosynthesis in subtropical Hawaiian waters. *Mar. Biol.*, **76**, 203–211 https://doi.org/10.1007/BF00392736.

Taniguchi, D. A. A., Franks, P. J. S. and Poulin, F. J. (2014) Planktonic biomass size spectra: an emergent property of size-dependent physiological rates, food web dynamics, and nutrient regimes. *Mar. Ecol. Prog. Ser.*, **514**, 13–33 https://doi.org/10.3354/meps10968.

Taylor, D. I. and Allanson, B. R. (1995) Organic carbon fluxes between a high marsh and estuary, and the inapplicability of the outwelling hypothesis. *Mar. Ecol. Prog. Ser.*, **120**, 263–270 https://www.doi.org/10.3354/meps120263.

Teichberg, M., Fox, S. E., Olsen, Y. S., Valiela, I., Martinetto, P., Iribarne, O., Muto, E. Y., Petti, M. A., *et al.* (2010) Eutrophication and macroalgal blooms in temperate and tropical coastal waters: nutrient enrichment experiments with *Ulva* spp. *Glob. Change Biol.*, **16**, 2624–2637 https://www.doi.org/10.1111/j.1365-2486.2009.02108.x.

Therriault, J.-C. and Platt, T. (1981) Environmental control of phytoplankton patchiness. *Can. J. Fish. Aquat. Sci.*, **38**, 638–641 https://doi.org/10.1139/f81-085.

Tomas, C. R. (1997) *Identifying Marine Phytoplankton*, Academic Press, New York.

Traut, B. H. (2005) The role of coastal ecotones: a case study of the salt marsh/upland transition zone in California. *J. Ecol.*, **93**, 279–290.

Tzortziou, M., Neale, P. J., Osburn, C. L., Megonigal, J. P., Maie, N. and Jaffé, R. (2008) Tidal marshes as a source of optically and chemically distinctive colored dissolved organic matter in the Chesapeake Bay. *Limnol. Oceanogr.*, **53**, 148–159 https://doi.org/10.4319/lo.2008.53.1.0148.

Utermöhl, H. (1958) Zur Vervollkomnung der quantitativen Phytoplankton-methodik. *Mitt. Int. Ver. Theor. Amgewan. Limnol.*, **9**, 1–38.

Venrick, E. L. (1978) How many cells to count? In Sournia, A. (ed.), *Phytoplankton Manual*, UNESCO, Paris, France.

Villafañe, V. E., Barbieri, E. S. and Helbling, E. W. (2004) Annual patterns of ultraviolet radiation effects on temperate marine phytoplankton off Patagonia, Argentina. *J. Plankton Res.*, **26**, 167–174 https://doi.org/10.1093/plankt/fbh011.

Walsh, J. J. (1981) Shelf-sea ecosystems. In Longhurst, A. R. (ed.), *Analysis of Marine Ecosystems*, Academic Press, New York, pp. 159–196.

Wang, H., Hsieh, Y. P., Harwell, M. A. and Huang, W. (2007) Modeling soil salinity distribution along topographic gradients in tidal salt marshes in Atlantic and gulf coastal regions. *Ecol. Model.*, **201**, 429–439 https://doi.org/10.1016/j.ecolmodel.2006.10.013.

Williams, G. N., Dogliotti, A., Zaidman, P., Solis, M., Narvarte, M. A., González, R. C., Esteves, J. L. and Gagliardini, D. A. (2013) Assessment of remotely-sensed sea-surface temperature and chlorophyll-a concentration in San Matías gulf (Patagonia, Argentina). *Cont. Shelf Res.*, **52**, 159–171 http://www.doi.org/10.1016/j.csr.2012.08.014.

Zedler, J. B., Callaway, J. C., Desmond, J. S., Vivian-Smith, G., Williams, G. D., Sullivan, G., Brewster, A. E. and Bradshaw, B. K. (1999) Californian salt-marsh vegetation: an improved model of spatial pattern. *Ecosystems*, **2**, 19–35 https://doi.org/10.1007/s100219900055.

Zohary, T. and Ashton, P. J. (1985) The effects of design and operation on the efficiency of hosepipes as water column samplers for phytoplankton. *J. Limnol. Soc. Sth. Afr.*, **11**, 5–10 https://doi.org/10.1080/03779688.1985.9633102.